UNIVERZITA KARLOVA

V PRAZE

Přírodovědecká fakulta

Katedra fyzikální a makromolekulární chemie

BAKALÁŘSKÁ PRÁCE

Ab initio nonadiabatic molecular dynamics simulation of Na_3F and azobenzene molecules

(Ab initio simulace neadiabatické molekulové dynamiky molekul Na_3F a azobenzenu)

Vypracoval: Marek Pederzoli

Vedoucí bakalářské práce: Mgr. Jiří Pittner Dr. rer. nat.

Studijní program: Chemie

Studijní obor: Chemie v přírodních vědách

Prohlášení

Prohlašuji, že jsem tuto bakalářskou práci vypracoval samostatně, pod vedením školitele Mgr. Jiřího Pittnera Dr. rer. nat. a že jsem všechny použité prameny řádně citoval.

Jsem si vědom toho, že případné využití výsledků, získaných v této práci, mimo Univerzitu Karlovu v Praze a pracoviště vedoucího práce, Ústavu fyzikální chemie J. Heyrovského AV ČR, je možné pouze po písemném souhlasu těchto institucí.

V Praze dne……

…….

podpis

ABSTRACT

Ab initio nonadiabatic molecular dynamics is a relatively new and modern approach for describing the time evolution and time-dependent properties of molecular systems, which cannot be described employing neither simple force field methods nor quantum chemical methods limited by the Born-Oppenheimer approximation. This approach is particularly needed for study of systems important in photochemistry, where excited states and crossings between potential energy surfaces are essential in the reaction mechanisms.

Because the full quantum treatment is accessible only for the smallest systems, approximations have to be employed. In this work, we present ab initio molecular dynamics of two molecular systems using the newly implemented approximate method based on wave function overlaps.

On the example of Na_3F cluster, we shall introduce the new methods for approximating the nonadiabatic coupling terms. Some of these approximative methods were later used in our study of azobenzene cis-trans photoisomerization, which is a very important reaction with many useful applications. Despite many previous works, the exact mechanism of the reaction is not completely clear yet. The newly developed approximative approaches allow us to use more accurate quantum chemical methods that will hopefully enable us to address some of the unanswered questions and confirm (or disprove) previous results obtained by semi-empirical methods.

SOUHRN

Neadiabatická ab initio molekulová dynamika je relativně novým a moderním přístupem pro popis časového vývoje a časově závislých vlastností molekulárních systémů, které není možné popsat pomocí jednoduché parametrizované molekulové mechaniky ani pomocí metod kvantové chemie, které jsou limitovány oblastí platnosti Born-Oppenheimerovy aproximace. Tento přístup je obzvláště nutný při studiu fotochemicky významných systémů, pro něž jsou excitované stavy a oblasti křížení povrchů potenciální energie při popisu reakčních mechanismů klíčové.

Jelikož je plně kvantový popis dostupný pouze pro velmi malé systémy, je nutno aplikovat různé aproximace. V této práci popíšeme ab initio molekulovou dynamika dvou různých molekulárních systémů s použitím nově implementovaných přibližných metod založených na překryvech vlnových funkcí.

Na příkladu klastru Na_3F ukážeme nové metody pro aproximaci neadiabatických couplingových členů. Některé z těchto aproximací budou použity také následující studii fotoisomerizační reakce azobenzenu, což je velmi důležitá reakce s mnoha užitečnými aplikacemi. I přes intenzivní výzkum není mechanismus této reakce ještě zcela objasněn.

Nově vyvinuté aproximativní metody nám dovolují použití přesnějších kvantově chemických metod, pomocí nichž se nám, doufejme, podaří odpovědět na některé dosud nezodpovězené otázky a ověřit (či vyvrátit) předchozí závěry plynoucí ze semi-empirických studií.

ACKNOWLEDGEMENT

I would like to express my gratitude to all those who gave me the possibility to complete this thesis. In this place, I would like to thank my supervisor Mgr. Jiří Pittner Dr. rer. nat. for his help and patience. I also thank the members of the group in Vienna, mainly Professor Hans Lischka and Priv.-Doz. Dr. Mario Barbatti, and also all my colleagues for their assistance and help with various little (and sometimes larger) problems I encountered during my work.

INDEX

1 INTRODUCTION

More than half a century already passed since first molecular dynamics calculations have been carried out [1]. Since that time, the field of molecular dynamics has been expanding very rapidly and it has influenced many branches of science. This fast progress is mainly caused by the unstoppable growth of the power of modern computers: the calculations that took long hours on the best supercomputer in Los Alamos in the 50s can be nowadays finished in a matter of seconds.

In spite of the incredible advance of computational power accompanied by new efficient algorithms and very sophisticated theories that together allowed achieving astonishing accuracy when treating small molecules, there is still much work to be done for describing larger systems.

In this work, I will describe some of the modern techniques of molecular dynamics and apply them on two different systems: the cluster Na3F and azobenzene molecule.

The Na3F cluster is interesting mainly from the theoretical point of view. The small size allowed using very accurate quantum chemical methods. The practical simulation of its pump-probe femtosecond spectrum has been successfully compared with experiment [2]. On this system, we tested and compared the results of two newly implemented methods for approximate calculation of the nonadiabatic coupling terms.

On the other hand, azobenzene photoisomerization reaction has many real world applications and many more new ones have been proposed. A full understanding of the mechanism of this reaction is therefore of great importance, particularly for some of the future applications.

We address the problem of the photoisomerization mechanism with an ab initio nonadiabatic dynamics simulation on CI/CASSCF level using the newly implemented efficient algorithm for calculation of the nonadiabatic couplings.

In the next section, the main theoretical aspects of the methods employed in this work are explained. The section starts with the Born-Oppenheimer approximation (BOA), which plays a central role in many methods of quantum chemistry. A detailed explanation of this approximation will be given while introducing some notions that will be used later in the text. Also, the limitations of BOA will be described because later in this work we will go beyond this approximation. The theory section then continues with the brief description of the ab initio methods used, followed by an introduction to molecular dynamics, and closing with a description of methods for nonadiabatic dynamics and approximate calculation of nonadiabatic couplings.

2 THEORETICAL PART

2.1 BORN OPPENHEIMER APPROXIMATION

The non-relativistic quantum chemistry aims at solving the Schrödinger equation:

$$\hat{H}\Psi = \mathrm{E}\Psi, \tag{1}$$

where Ψ is the wave function, H is the Hamiltonian (operator of the total energy) and E its eigenvalue. The Hamiltonian can be written as:

$$\hat{H} = -\frac{1}{2}\sum_i \nabla_i^2 - \sum_A \frac{1}{2M_A}\nabla_A^2 - \sum_{A,i}\frac{Z_A}{r_{Ai}} + \sum_{A>B}\frac{Z_A Z_B}{R_{AB}} + \sum_{i>j}\frac{1}{r_{ij}}, \tag{2}$$

where atomic units are used. The terms are in this order: The kinetic energy of the electrons, the kinetic energy of the nuclei, Coulombic interactions of electrons with nuclei, Coulombic interactions of nuclei, and Coulombic interactions of electrons. More compactly:

$$\hat{H} = \hat{T}_{\mathrm{N}}(\boldsymbol{R}) + \hat{T}_{\mathrm{e}}(\boldsymbol{r}) + \hat{V}_{\mathrm{eN}}(\boldsymbol{r},\boldsymbol{R}) + \hat{V}_{\mathrm{NN}}(\boldsymbol{R}) + \hat{V}_{\mathrm{ee}}(\boldsymbol{r}), \tag{3}$$

where the terms are in the same order corresponding to equation (2).

The Schrödinger equation with the Hamiltonian in this form is impossible to solve analytically even for smallest molecules, therefore approximations must be taken.

Born and Oppenheimer [3] in 1927 showed that the separation of electronic and nuclear motion is possible. This separation is intuitive considering the difference in mass of the nuclei and electrons. We can imagine that the very slow nuclei create stationary field in which the electrons move and on the other hand, the nuclei move in a field created by averaging the fast movement of the electrons. This separability corresponds to the wave function ansatz in the form:

$$\Psi_{\mathrm{total}} = \Psi_{\mathrm{electronic}} \times \Psi_{\mathrm{nuclear}}\ . \tag{4}$$

This is also the basic idea of the so-called Born-Oppenheimer approximation (BOA).

In this work, we will be dealing with systems in which BOA does not hold so let's take a more rigorous look on this approximation and its limits.

Let's assume that we can solve the electronic problem

$$\hat{H}_{\mathrm{el}}\Psi(\mathbf{r};\mathbf{R}) = \mathrm{E}_{\mathrm{el}}\Psi(\mathbf{r};\mathbf{R}), \tag{5}$$

which is the Schrödinger equation without electron-nuclear interaction. The electronic Hamiltonian has the form:

$$\hat{H}_{\mathrm{el}} = \hat{T}_{\mathrm{e}}(\boldsymbol{r}) + \hat{V}_{\mathrm{eN}}(\boldsymbol{r},\boldsymbol{R}) + \hat{V}_{\mathrm{NN}}(\boldsymbol{R}) + \hat{V}_{\mathrm{ee}}(\boldsymbol{r}). \tag{6}$$

It can be shown that the solutions Ψi form a complete basis set. We can expand the solution of (1) as:

$$\Psi(\mathbf{r};\mathbf{R}) = \sum_k \Psi_k(\mathbf{r};\mathbf{R})\chi_k(\boldsymbol{R}), \tag{7}$$

where χ_k are the expansion coefficients. After substituting (7) into (1) and multiplying by Ψ_l we obtain

$$\left[\hat{T}_{\mathrm{N}} + E_k^{\mathrm{el}}(\boldsymbol{R}) - E\right]\chi_k(\boldsymbol{R}) = \sum_l \hat{B}_{kl}\chi_l(\boldsymbol{R}), \tag{8}$$

where operators $\hat{B}_{kl}$ are defined as:

$$\hat{B}_{kl} = \sum_A \frac{1}{M_A}\left[\left\langle\phi_k(\boldsymbol{r};\boldsymbol{R})\middle|\boldsymbol{\nabla}_{\mathrm{R}_A}\middle|\phi_l(\boldsymbol{r};\boldsymbol{R})\right\rangle_r \boldsymbol{\nabla}_{\mathrm{R}_A} + \frac{1}{2}\left\langle\phi_k(\boldsymbol{r};\boldsymbol{R})\middle|\boldsymbol{\nabla}^{\boldsymbol{2}}_{\mathrm{R}_A}\middle|\phi_l(\boldsymbol{r};\boldsymbol{R})\right\rangle_r\right]. \tag{9}$$

The system of equations (7) is exact and the matrix $\boldsymbol{B} = \hat{B}_{kl}$ represents the coupling between electronic and nuclear motions. This is equivalent to (1) and it is similarly hard to solve (it has not been solved analytically for any system more complex than H^{2+} [4]). If we neglect all the off-diagonal terms of **B** we get the following set of equations:

$$\left[\hat{T}_{\mathrm{N}} + \hat{U}_k(\boldsymbol{R})\right]\chi_k(\boldsymbol{R}) = E\chi_k(\boldsymbol{R}) \tag{10}$$

$$\hat{U}_k(\boldsymbol{R}) = E_k^{\mathrm{el}}(\boldsymbol{R}) - \hat{B}_{kk}, \tag{11}$$

where $\left[\hat{T}_N + \hat{U}_k(\boldsymbol{R})\right]$ can be interpreted as a nuclear Hamiltonian with $\hat{U}_k$ being the effective nuclear potential dependent on the nuclear coordinates. This approximation is called adiabatic and it allows the separation of nuclear and electronic motion while maintaining some of the interaction of both. It can be shown that the expression (6) in this approach becomes:

$$\Psi_{\mathrm{k},\upsilon}(\mathbf{r};\mathbf{R}) = \chi_{k,\upsilon}(\boldsymbol{R})\phi_k(\boldsymbol{r};\boldsymbol{R}). \tag{12}$$

Considering (4) we can see that the expansion coefficient χ_k has the meaning of nuclear wave-function. (The υ in (12) is the quantum number of the nuclear wave function, see [5] for more details.)

Usually one neglects also the diagonal terms in **B** matrix. This is called the Born-Oppenheimer approximation and it yields:

$$\left[\hat{T}_N + E_k^{\mathrm{el}}(\boldsymbol{R})\right]\chi_k(\boldsymbol{R}) = E\chi_k(\boldsymbol{R}). \tag{13}$$

It has been shown [6] that the energy calculated using the BOA is the lower limit to an exact value E.

Let's have a look at conditions of validity of BOA. In the framework of Rayleigh-Schrödinger perturbation theory, we can assume the BOA as the zeroth order approximation, the diagonal correction $\hat{B}_{kk}$ as the first order perturbation and the off-diagonal terms $\hat{B}_{kl}$ as the second order perturbation. From the convergence criterion of the perturbation expansion it can be shown that the adiabatic approximation is valid if [4]:

$$\left\langle \chi_{k,\mu}(\boldsymbol{R})\middle|\hat{B}_{kl}\middle|\chi_{l,\nu}(\boldsymbol{R})\right\rangle \ll \left|E_{k,\mu} - E_{l,\nu}\right|, \tag{14}$$

this inequality is not fulfilled when the potential energy surfaces are close, i.e. near avoided crossing, crossing seams and conical intersections.

2.2 AB INITIO METHODS

The term Ab initio (lat. "from the beginning") denotes the whole range of quantum chemical methods in which no empirical data are used for approximately solving the electronic Schrödinger equation (5).

2.2.1 Hartree-Fock method

The Hartree Fock (HF) method is the most basic ab initio method for treating molecular systems. Today it is mainly used as a first guess for more advanced, so-called post-Hartree-Fock methods. In this work, we will only need HF method for closed shells systems and by HF we actually mean restricted Hartree Fock method, RHF. The description of the open shell methods ROHF and UHF can be found in [7]

HF method is a variational method i.e. it obeys the variational principle stating:

$$E[\Phi] \geq E[\Psi_0] = \mathrm{E}_0, \tag{15}$$

where E_0 is the exact energy of the ground state, Φ is the trial function and $E[\Phi]$ is a functional in form:

$$E[\Phi] = \langle \widehat{H} \rangle_{\Phi} = \frac{\langle \Phi | \hat{H} | \Phi \rangle}{\langle \Phi | \Phi \rangle}. \tag{16}$$

Simply put, the variational principle states that any energy computed using a trial wavefunction is never smaller than the exact energy of the ground state (see [8] for a proof and more rigorous description).

It can be shown [7], that minimizing the electronic energy of the system that is described by one Slater determinant (an antisymetrized product of spin-orbital) leads to the Hartree-Fock equations in canonical form:

$$f|\chi_a\rangle = \varepsilon_a|\chi_a\rangle, \tag{17}$$

where $\hat{f}$ is the Fock operator

$$\hat{f}(1) = -\frac{1}{2}\nabla_1^2 - \sum_A \frac{Z_A}{r_{1A}} + \sum_b^N \left[\hat{J}_b(1) - \widehat{K}_b(1)\right], \tag{18}$$

and J and K are the Coulomb and the exchange operators

$$\hat{J}_b(1)\chi_a(1) = [\int dx_2 \chi_b^*(2) r_{12}^{-1} \chi_b(2)]\chi_a(1) \tag{19}$$

$$\hat{K}_b(1)\chi_a(1) = [\int dx_2 \chi_b^*(2) r_{12}^{-1} \chi_a(2)]\chi_b(1). \tag{20}$$

Equations (17) are integro-differential equations that are very hard to solve analytically, but it turns out that they can be transformed into algebraic Roothaan-Hall equations employing a finite Gaussian basis$\{\phi_\mu\}$:

$$\boldsymbol{FC} = \boldsymbol{SC\epsilon} \tag{21}$$

$$S_{\mu\nu} = \int d\boldsymbol{r} \phi_\mu^*(1)\phi_\nu(1) \tag{22}$$

$$F_{\mu\nu} = \int d\boldsymbol{r} \phi_\mu^*(1)\hat{f}(1)\phi_\nu(1), \tag{23}$$

where **S** is the overlap matrix, **C** is the matrix of LCAO coefficients, **ε** is the diagonal matrix of orbital energies, and **F** is the Fock matrix. We can see that the Fock matrix also depends on the actual wave functions so these equations have to be solved iteratively. The procedure of diagonalizing the Fock matrix and constructing a new one based on the new orbital is repeated until self-consistency is achieved (HF method is also known as a self consistent field method, SCF).

There are several approximation considered in the HF approach:

1) The Born-Oppenheimer approximation
2) The variational solution is assumed to be a linear combination of finite number of atom-centered Gaussian basis function.
3) The Hamiltonian ground state eigenfunction is assumed to be described by a single Slater determinant.

The HF method serves a reference for a definition of correlation energy, which is defined as the difference between HF limit after extrapolating to an infinite basis and the exact non-relativistic energy.

2.2.2 Multi-configurational self-consistent field

Multi-configurational self-consistent field (MCSCF) is a variational method of quantum chemistry, which uses a linear combination of configuration state functions (CSFs, each being a symmetry- and spin-adapted linear combination of Slater determinants) to approximate the exact electronic wavefunction. In a way, it is a generalization of the HF method, which only uses one Slater determinant, and it offers the most general approach to the computation of chemical reactions and multiple electronic states. [9]

Let's take a look at a simple example of how MCSCF wavefunction is constructed. Let's consider methylene CH_2. The highest occupied molecular orbital of methylene, which we shall denote a_1, is a mixture of 2s and $2p_z$ atomic orbital at a bent HCH angle but as the angle opens the $2p_z$ character raises and 2s character diminishes to zero as the angle reaches 180 degree. The loss of 2s character also raises the energy of the orbital. The lowest unoccupied molecular orbital, which we will denote b_1, is pure carbon $2p_z$ orbital so both molecular orbital become degenerate when the molecule becomes linear.

For a bent configuration, the ground state is a singlet state, which can be well described by putting the two electrons in a_1 and first excited triplet state by putting one of the electrons in each MO. This qualitatively correct solution can be obtained with single-configuration wave function with HF method. For the ground state (singlet), we get:

$$\Psi = a_1(\alpha)a_1(\beta) \tag{24}$$

and for the first excited state (triplet) using RHF we can obtain:

$$\Psi_{RHF} = a_1(\alpha)b_1(\beta). \tag{25}$$

Let's see what happens when we open up the HCH angle. While the triplet state description stays correct, the singlet state description becomes incorrect quickly as the configuration with both electrons in b_1 becomes more important. As the molecule becomes linear, the qualitatively correct wavefunction is

$$\Psi = \frac{1}{\sqrt{2}}[a_1(\alpha)a_1(\beta) + b_1(\alpha)b_1(\beta)]. \tag{26}$$

It is clear that the wavefunction that qualitatively describes the bending of HCH should be in form:

$$\Psi = A[\mathrm{a}_1(\alpha)\mathrm{a}_1(\beta)] + B[\mathrm{b}_1(\alpha)\mathrm{b}_1(\beta)], \tag{27}$$

where A and B are variational parameters.

For more complicated systems, there have been arguments about how to choose the important configuration. It turned out that one of the best (and certainly the most consistent) ways is to include all configurations, which arise from distributing all the active electrons among the active orbitals. This approach is known as the complete active space SCF (CAS-SCF) [10] or as full-optimized reaction space (FORS) MCSCF [11].

2.2.3 Configuration interaction

Configuration interaction is another variational post-Hartree-Fock method, which in order to account for the electron correlation uses a linear combination of Slater determinants/configuration state functions Φ_I

$$\Psi = \sum_I c_I \Phi_I. \tag{28}$$

If the sum in equation (28) includes all possible CSFs (of appropriate symmetry), then the method is called full CI. This methods yields exact solution of the electronic Schrödinger equation within the space spanned by the orbital basis set.

Although the full CI calculation represents an exact solution within the finite basis set approach, they are not used except for very small systems because the computational cost scales very fast [12]:

$$\mathrm{O}^{\mathrm{FCI}} = N_{\mathrm{det}} N^2 n^2, \tag{29}$$

where N is the number of electrons, n the number of spin orbital, N_{det} is the number of determinants equal to $\binom{n}{N}$. The number of configuration has to be lowered considerably for bigger systems.

The term Φ_0 is the reference state (usually the ground state) and all the determinants that differ in only one spin orbital are described as single excitations and analogically for higher exci-

tations. If we only include the single excitations than the method is called CI singles (CIS) and analogically CISD includes all the single and double excitations.

In this work, we use a multireference version of this method (MR-CI). As the name suggests, in this method the determinants are generated as excitations from several references, usually obtained from CASSCF.

2.3 MOLECULAR DYNAMICS

2.3.1 Basic concepts

Molecular dynamics can be defined as a computer simulation of the behavior of molecules and atoms in time. [13] There are many types of molecular dynamics simulations. One big group of methods is used to compute various physical quantities by methods of statistical thermodynamics. These methods use very large ensembles of molecules and long trajectories. On the other hand, there are simulations of individual molecules (like the ones described in this work) which are used in investigation of reaction mechanisms and simulation of time dependent experiments like pump-probe femtosecond spectroscopy.

Probably the most important decision to be made when attempting to use molecular dynamics is the choice of the level of theory used to describe the system under study. Usually one has to make some compromise between accuracy and computational cost.

Even for very small molecules, a full quantum mechanical treatment is extremely time demanding. Usually the nuclei are treated classically i.e. equations of classical mechanics are used (and possibly some semi-classical approaches are then employed). The Newton equations:

$$m_i \frac{d^2 r_i}{dt^2} = f_i = -\nabla_{r_i} V \tag{30}$$

are the most common, since they are the simplest, but sometimes more general approaches like Langrangian and Hamiltonian mechanics are used.

There are also many approaches to solving these equations. One of the most often used is the Verlet algorithm [14]:

$$\vec{r}(t + \Delta t) = 2\vec{r}(\Delta t) - \vec{r}(t - \Delta t) + \vec{a}(t)\Delta t^2 \tag{31}$$

$$\vec{v}(t) = \frac{[\vec{r}(t+\Delta t)-\vec{r}(t-\Delta t)]}{2\Delta t}, \tag{32}$$

alternatively, a slightly modified version, velocity Verlet:

$$\vec{r}(t+\Delta t) = \vec{r}(\Delta t) + \vec{v}(t)\Delta t + \frac{\vec{a}(t)\Delta t^2}{2} \tag{33}$$

$$\vec{v}(t+\Delta t) = \vec{v}(t) + \frac{\vec{a}(t)+\vec{a}(t+\Delta t)}{2}\Delta t. \tag{34}$$

The initial conditions at t = 0 (positions and velocities) of the atoms have to be specified and the length of the time step Δt selected for an ensemble of trajectories. Than based on the level of theory used various techniques are carried out to calculate what the positions and velocities will be in time t = Δt. This procedure is repeated to the end of the trajectory for a defined number of steps.

For calculating the potential there are much more possibilities to choose from. The simplest way, called molecular mechanics, is to break down the potential into two-body, three-body (and higher) contributions and parameterize these contributions empirically.

In ab initio molecular dynamic the ab initio methods briefly described in section 2.2 are used. The potential surfaces can be computed either in advance or on the fly. Both approaches have their pros and cons. If the surfaces are computed beforehand the trajectories themselves are very fast and also much information can be gained just by investigating the surfaces alone, however this is only profitable for smallest systems. The "on the fly" approach on the other hand allows running trajectories through very complicated surfaces that would take extremely long to precalculate completely.

2.3.2 Methods of nonadiabatic molecular dynamics

As we already mentioned not all systems can be correctly described using the BOA, in particular it breaks down when the potential energy surfaces come close together.

Because the solution of electron-nuclear dynamics would require a quantum treatment of the nuclei, we need some method that can account for the coupling terms in the framework of classical mechanics trajectories.

There are several approximate methods to include the nonadiabatic effect into classical molecular dynamics including variations of Ehrenfest method [15], various version of surface hopping [16], multiple spawning method [17] and others.

In this work we will be using Tully's surface hopping [18] method briefly described below.

The main idea on Tully's method is that the nuclei always move on a single potential energy surface (as in BOA) but they are allowed to switch the surface when necessary (this is referred to as performing a "hop" or "hopping").

After expanding the electronic wave function in the basis of geometry-dependent adiabatic states with time dependent coefficients

$$\phi(t) = \sum_j c_j(t)\,\phi_j\big(\boldsymbol{R}(t)\big). \tag{35}$$

The following equation for the coefficients can be obtained:

$$i\dot{c}_k(t) = \sum_j \left[E_j\,\delta_{kj} - i\dot{\boldsymbol{R}}(t)\cdot\langle\phi_k|\nabla_{\mathbf{R}}|\phi_j\rangle\right] c_j(t) \tag{36}$$

The hopping probability is proportional to the variation of the quantum populations usually with the additional constraint that the number of hopping events is minimized (this is called the least switches approach) [16].

The hopping probabilities can be calculated as follows:

$$g_{kj} = \frac{\Delta t\,\boldsymbol{b}_{jk}}{c_k c_k^*}, \tag{37}$$

where

$$\mathbf{b}_{jk} = 2Im(c_k^* c_l E_k \delta_{kl}) - 2Re\left(c_k^* c_l \dot{\boldsymbol{R}}(t)\right)\cdot\langle\phi_k|\nabla_{\mathbf{R}}|\phi_l\rangle, \tag{38}$$

where $\langle\phi_k|\nabla_{\mathbf{R}}|\phi_l\rangle$ is the nonadiabatic coupling vector for the adiabatic states k and l. The scalar product of $\langle\phi_j|\nabla_{\mathbf{R}}|\phi_k\rangle$ with velocities **v** expresses the nonadiabatic coupling between the adiabatic surfaces j and k.

The algorithm of the surface hopping dynamics looks like this:

1) For a nuclear geometry at a given time step the electronic Schrödinger equation is solved. Energy, gradient and nonadiabatic coupling vector are calculated.

2) The gradient of the current potential energy surface is used to update the nuclear geometry according to Newton equations using the Verlet algorithm.
3) The coefficients $c_j(t)$ are propagated using the time dependent Schrödinger equation and the hopping probabilities g_{kj} are computed.
4) If a "hop" is performed then the velocities are adjusted to conserve energy.
5) The procedure 1) to 4) is repeated over and over until the end of the trajectory
6) Whole ensemble of trajectories is computed to obtain the "classical wave packet".

One of the most time consuming steps in surface hopping procedure is calculation of the nonadiabatic coupling terms at CASSCF or CI level.

2.3.3 Approximate methods for calculation of nonadiabatic couplings

The approximation that we use and which has been recently implemented to Newton X package was proposed by Hammes-Schiffer and Tully and later by Rothlisberger et al. [19]

The main idea is to replace the analytic nonadiabatic couplings by time-derivatives obtained as finite differences between time steps:

$$\frac{d\boldsymbol{R}}{dt}\left(t+\frac{\Delta t}{2}\right)\cdot\langle\phi_k|\nabla_{\mathbf{R}}|\phi_j\rangle\left(t+\frac{\Delta t}{2}\right)\approx$$
$$\frac{1}{2\Delta t}[\langle\phi_k(\boldsymbol{R}(t))|\phi_j(\boldsymbol{R}(t+\Delta t))\rangle-\langle\phi_k(\boldsymbol{R}(t+\Delta t))|\phi_j(\boldsymbol{R}(t))\rangle. \quad (39)$$

In this approach, we do not obtain the individual couplings themselves but rather their scalar product with velocity, which is however sufficient for the Tully hopping method described before.

The overlaps between MCSCF/MR-CI wave functions in equation (39) are much easier to calculate than the nonadiabatic couplings; however, for a large MR-CI they have worse computational scaling. This problem can be effectively solved by limiting excitation levels and numerical thresholding. Finally, CI wave function overlaps can be reduced to calculating overlaps between molecular orbitals at different geometries [20].

Another method for dealing with nonadiabatic effects was described by Granuci, Persico, and Toniollo [21]. They introduced a locally diabatic basis η, in which the scalar product $\frac{d\boldsymbol{R}}{dt}(t)\cdot\langle\eta_k|\nabla_{\mathbf{R}}|\eta_j\rangle$ vanishes. The diabatic basis is related to the adiabatic electronic states by a

unitary transformation $\boldsymbol{T}(\boldsymbol{R}(t))$, different in each time step. It has been shown that the transformation matrix can be obtained from the overlaps of the adiabatic wave function by means of Lödwin ortogonalization:

$$\boldsymbol{T} = \boldsymbol{S}(\boldsymbol{S}^T\boldsymbol{S})^{-1/2}. \tag{40}$$

The knowledge of the **T** matrix then allows transforming the Hamiltonian to the diabatic basis, propagating the expansion coefficients $c_k(t)$ in the diabatic basis, transforming them back to the adiabatic one, and computing the surface hopping probabilities in a similar way as in the original Tully's method.

2.4 STUDIED SYSTEMS

2.4.1 Na_3F

The Na_3F cluster is one of the whole range of NaF clusters previously theoretically investigated by several authors. [22, 23]

The electronic structure, absorption spectrum and also the ionization potential are highly geometry dependent [24] and the ionization potential of different isomers of the same cluster may differ considerably. This allows monitoring selectively the passage through one specific isomer in time-resolved experiments. Also, the ionization probability may become time-dependent, provided the probe pulse energy is low enough to photoionize only one isomer while the molecule is vibrationally excited in such a way that it wanders through several structures.

Na_3F has two isomers (See figure 2), which have a vertical ionization energy that differs by almost 0.5 eV. The lowest isomer is a quasi-planar C_{2v} structure with vertical ionization energy of roughly 4.9 eV, while the higher one is a 3D C_{3v} structure. This second isomer lies slightly higher in energy (~65 meV above the first one) and has vertical ionization energy of 4.4 eV. The ground state of the cation is linear and the adiabatic ionization potential is 4.26 eV [24].

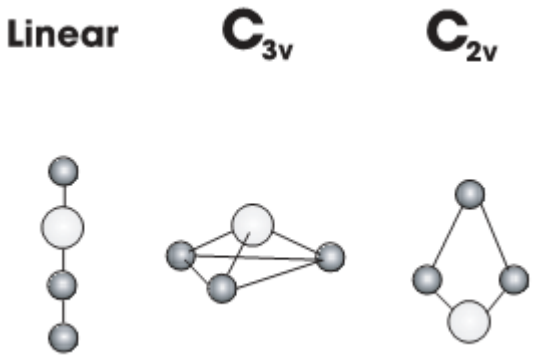

Figure 2

2.4.2 Azobenzene

Azobenzene undergoes an exceptionally clean cis-trans photochemical isomerization (see figure 3) after excitation to the $S_1(n,\pi^*)$ and the $S_2(\pi,\pi^*)$ states, which provides the basis for many applications including photomechanical energy conversion, light triggered switches and image storage devices, just to name a few of them. In spite of a number of previous theoretical works on azobenzene [25-29], there are still many unanswered questions about the mechanisms of this reaction. Having the possibilities to verify results of new methods by a comparison with previous works, yet being able to discover new important facts about azobenzene photochemistry makes this system an ideal case for testing new approaches and methods.

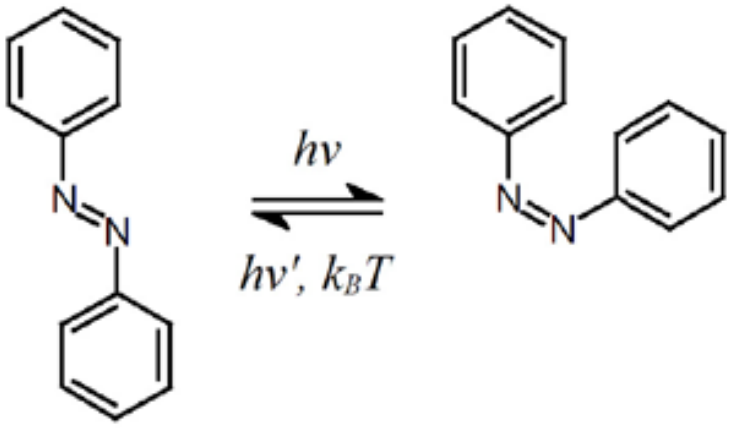

Figure 3

There are three suggested possible reaction pathways:

1) rotation (CNNC torsion),
2) inversion (N-N bending) and
3) "concerted inversion" [28] (simultaneous CNN bending).

On the ground state the inversion mechanism dominates.

After n-π excitation (S_1 state), only the rotation path is open via the conical intersection between S_1 and S_0 (see figure 4).

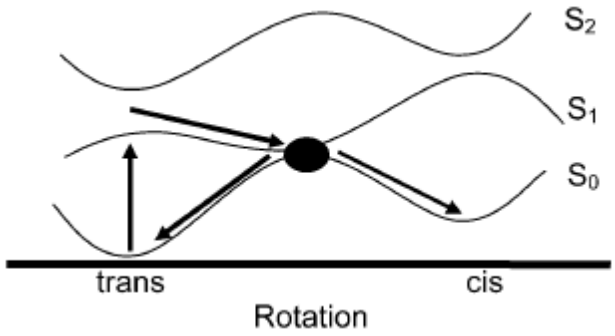

Figure 4

There might be, howewer, one or more other conical intersections between S0 and S1 some of which may be not accesible directly.

The mechanism of the isomerization after π-π excitation (S_2 state) is not clear yet.

It is generally agreed [26, 29] that the isomerization is unlikely to happen directly on the S_2 surface alone because of high barriers in all important directions. There are two possibilities how to get around this - relaxing to S_1 state or going through some intermediate state.

Most likely, the isomerization takes place on S_1. After the relaxation from higher state the molecule has more energy and it is on different place of the S1 surface so other reaction paths, different from the one after direct n-π* excitation, can be accessible. One possibility has been suggested by Diau [28]:

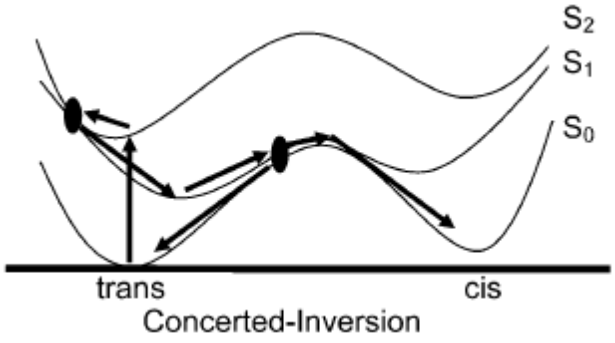

Figure 5

The most complete description of the mechanism so far has been done by Persico at al. [26] and it is based on semi-empirical molecular dynamics. Two conical intersections (CI) between S_2 and S_1 have been found. One CI on cis side, one on the trans side.

They suggest that after π-π^* excitation the molecule relaxes via S_2/S_1 CI and then it continues via the same S_1/S_0 CI as after direct n-π^* excitation via rotational pathway. This happens even faster because the geometry after relaxation from S_2 is a little closer to the S_2/S_1 CI than after exciting n-π^* directly.

It is also probable that higher states play an important role in the processes after π-π^* excitation [29]. The state $\pi\pi$-$\pi^*\pi^*$ seems to be of the greatest importance.

From the done discussion it is clear that there is a need for a new MD study on the ab initio level, which is able to quantitatively describe the process even if higher states are involved and if the wave function changes character in the process to verify previously mentioned results obtained by semi empirical-methods and clarify some of the uncertain aspects the dynamics of this important isomerization.

3 CALCULATIONS AND RESULTS

3.1 Na_3F

The main aim of this part of the work was to test the implementation of the new approximate treatment of nonadiabatic couplings in ab initio molecular dynamics.

All the simulations have been performed employing the Verlet program written by Dr. Pittner, which can carry out various important tasks, mainly surface hopping dynamics and geometry optimizations, but also conical intersection search etc.

The initial conditions created by means of the Wigner distribution for canonical ensemble at T=50K used in the previous study [2] have been employed.

The potential energy surfaces for ground and three lowest lying excited states were calculated on CISD level using the COLUMBUS package [30]. Only two excess electrons have been correlated (according to the frozen ionic bonds approximation [31]), thus effectively employing a full valence CI.

Effective core potential with polarization potential was used. The valence basis set 4s4p/3s3p for sodium and ECP with valence basis set 5s5p1d/4s4p1d for fluorine have been employed. This level of theory has been previously verified to yield reasonably accurate results. [32]

Since DALTON (which is used by COLUMBUS for generating the integrals) does not support ECP for gradient calculation, the ECP contribution to one-electron integrals and their derivatives had to be computed by the GAMES-UK program and inserted into the COLUMBUS calculation.

For treating the nonadiabatic effects the Tully's fewest switches surface hopping approach has been used.

Three sets of trajectories were run, each with a different method for dealing with nonadiabatic couplings. All three types of trajectories were 3000 steps long with a time step of 1 fs.

For the first set of trajectories the nonadiabatic couplings have been calculated analytically using the COLUMBUS package. Next set of trajectories used the Rothlisberger's method based on time derivatives and the last set used Persico's method of local diabatization procedure by a unitary transformation, which eliminates the explicit need of the coupling at all.

In total more than 40 trajectories have been ran while majority of them had to be submitted twice or more times because of random crashes of the trajectories on the old cluster which by that time had only three working computers.

In figure 4 a comparison of the three methods ran with same initial conditions can be seen.

All three methods have proved to be capable to describe the system and hopping between surfaces have been observed, but the low number of trajectories does not allow us to do a full statistical treatment in this case.

Because of lack of computer time on the cluster, where the program was installed, the methods were tested separately on other system, which allowed using 64-bit architecture and many times more computer power. The parallel tests were soon finished and published [20] so we discontinued the work on this system.

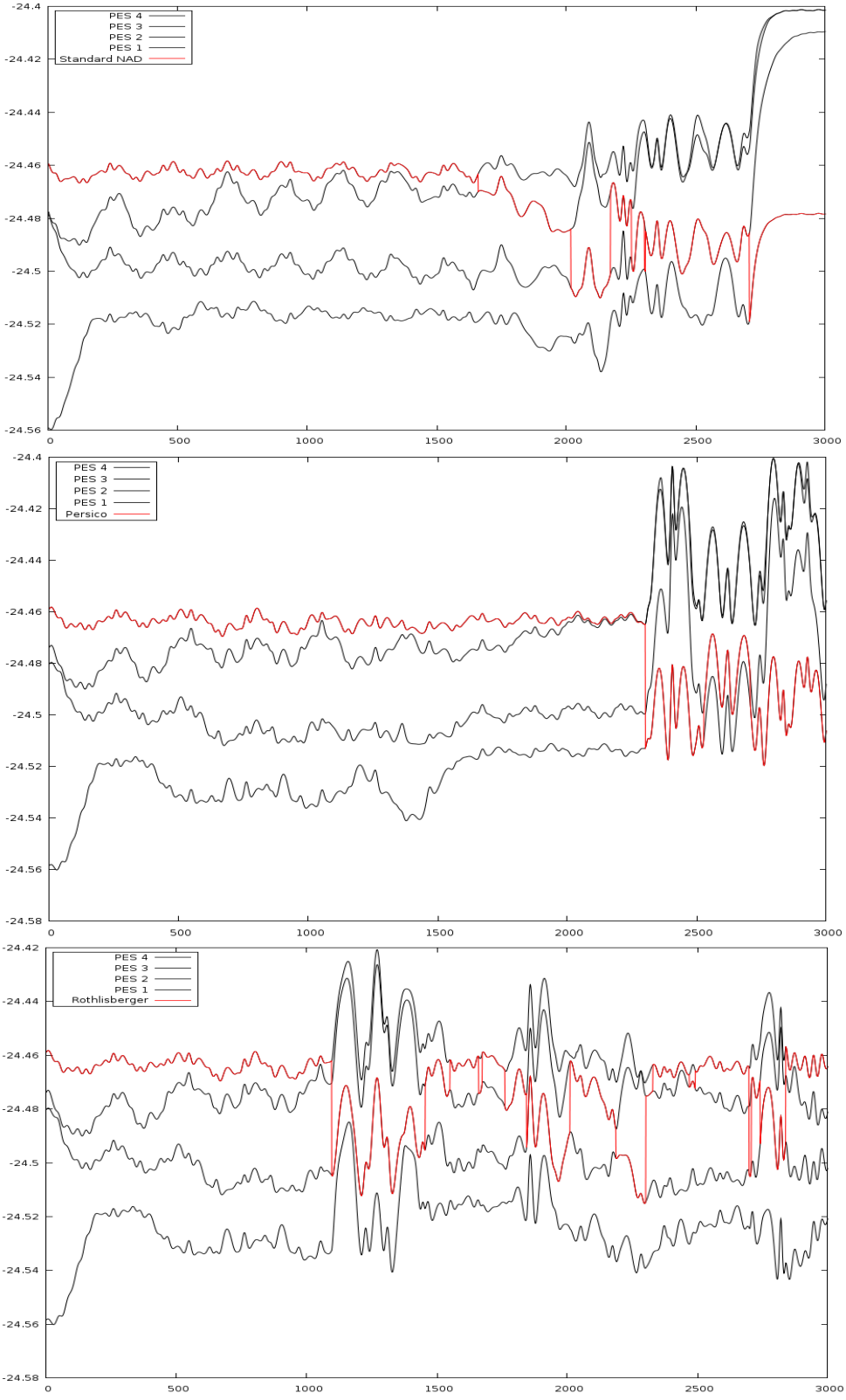

Figure 4: Comparison of three methods: Plot of energy [a.u.] vs. time [fs]

3.2 AZOBENZENE

In this section, we will describe the results of our work on the azobenzene cis-trans photoisomerization starting from the cis isomer after excitation to the S_1 state. This work is the first stage of a larger project aimed on azobenzene photoisomerization reaction. The goal of this project is to fully describe this isomerization after excitation to both S_1 and S_2 state, starting on both sides of the reaction and address some of the unanswered questions about the reaction mechanism that we mentioned earlier. The objectives for our first stage was to find an appropriate method for the ab initio dynamics, compare the results with previous studies and also verify the results obtained by semi-empirical methods [25].

The current work can be divided into two parts: the static calculations and the molecular dynamics simulations. We will discuss both separately.

3.2.1 Static calculations

The first part of our work was to choose the appropriate level of theory that is able to describe the system accurately but which is also fast enough to be used in a molecular dynamics simulation. Considering the fact that we are dealing with a system having a multiconfigurational character, we were left with MCSCF (CASSCF being the most reasonable and accessible choice of MCSCF) and MR-CIS methods (any higher excitations MR-CI would be too computationally demanding for molecular dynamics).

We carefully tested both approaches with single point calculations using the COLUMBUS package.

For CASSCF an active space of 10 electrons in eight orbitals was selected. This selection includes the two n orbitals on nitrogen atoms, π orbital on the NN bond, and two π orbitals of the benzene rings.

In table I we present the calculated vertical excitation energies compared with experimental values. It can be seen that the agreement with the experiment is reasonable. We tested various basis sets including the diffuse functions. Although the presence of diffuse functions lowered the vertical excitation energies in some cases, the results were not consistent and we decided not to use them at all (the diffuse functions lowered the energy of the Rydberg states too much, which was probably the cause of the inconsistency). The basis set used in the rest of this work is 6-31G

on carbon and hydrogen and 6-31G* for nitrogen atoms. In figure 5, we present a diagram of relative energy levels relevant for the isomerization after S_1 excitation.

Table I: Vertical excitation energies

Method	**Basis**	**E($S_{1\ cis}$)**	**E($S_{2\ cis}$)**	**E($S_{1\ trans}$)**	**E($S_{2\ trans}$)**
Target (exp)					
In solution [33]		2.87	4.42	2.8	3.89
In gas phase [34]		2.92	-	2.82	4.12
Present results					
SA2-CAS(10,8)	6-31G(C,H)/G*(N)	3.54	-	3.32	-
MR-CIS(4,3)	6-31G(C,H)/G*(N)	3.63	-	3.38	-
SA3-CAS(10,8)	6-31G(C,H)/G*(N)	3.36	5.53	3.24	6.18
MR-CIS(6,5)	6-31G(C,H)/G*(N)	3.43	5.38	3.31	5.40
MR-CIS(4,3)	6-31G(C,H)/G*(N)	2.69	4.61	3.42	5.49
SA3-CAS(10,8)	6-31G(C,H)/G*+s+p(N)	3.34	5.35	3.62	5.10
MR-CIS(4,3)	6-31G(C,H)/G*+s+p(N)	2.36	4.32	3.25	4.64
MR-CIS(6,5)	6-31G(C,H)/G*+s+p(N)	2.91	4.56	3.27	4.76
SA3-CAS(10,8)	6-31G(C,H)/G*+s(N)	3.56	5.50		
SA3-CAS(10,8)	6-31G(C,H)/G*+p(N)	3.67	5.61		

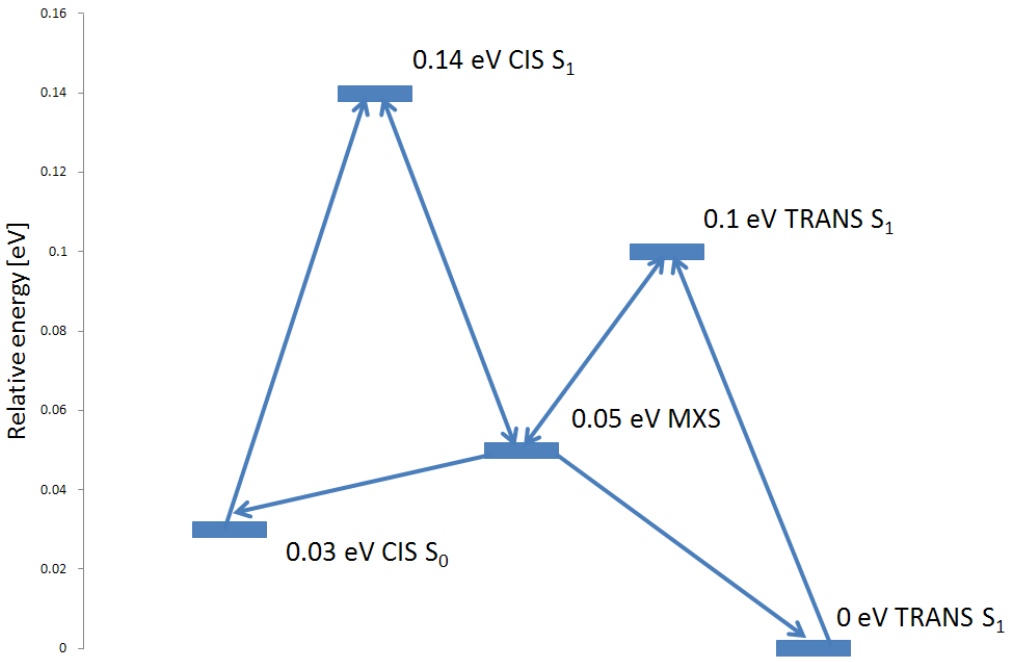

Figure 5 Diagram of energy levels relevant to the isomerization

Next part of the work was to optimize all the relevant structures and locate the conical intersections. We were able to optimize the ground and lowest two excited states for both isomers except of cis S_1 state, which probably does not have any real minimum.

We located one conical intersection between the ground and first excited state. This conical intersection is positioned in the middle of the rotational pathway in agreement with previous results. [25, 26, 27]

Table II contains the most important geometrical parameters of the optimized structures, (these parameters are the N-N and C-N distance, N-N-C angle, and C-N-N-C dihedral angle) and Figure 6 shows the structures.

Table II: Overview of the most important geometrical parameters of optimized structures

cis isomer	**N-N**	**N-C**	**N-N-C**	**C-N-N-C**
S_0 Exp,(X-ray)[35]	125.3	144.9	121.9	8
S_0 MR-CIS(4,3)	125.3	144.1	122	2
S_0 MR-CIS(5,6)	121.1	143.9	129/119	8
S_2 MR-CIS(4,3)	141.8	137.5	122	0
trans isomer	**N-N**	**N-C**	**N-N-C**	**C-N-N-C**
S_0 Exp,(X-ray)[35]	124.7	142.8	N/A	180
S_0 Exp,(GE)[36]	126	142.7	113.6	180
S_0 MR-CIS(4,3)	126	142.9	114	180
S_0 MR-CIS(5,6)	124.5	145	115/114	179
S_1 MR-CIS(4,3)	127.2	137.8	126	180
S_2 MR-CIS(4,3)	135.5	135	111	180
conical intersection	**N-N**	**N-C**	**N-N-C**	**C-N-N-C**
S_0/S_1 MR-CIS(4,3)	124.7	133/141	118/135	92

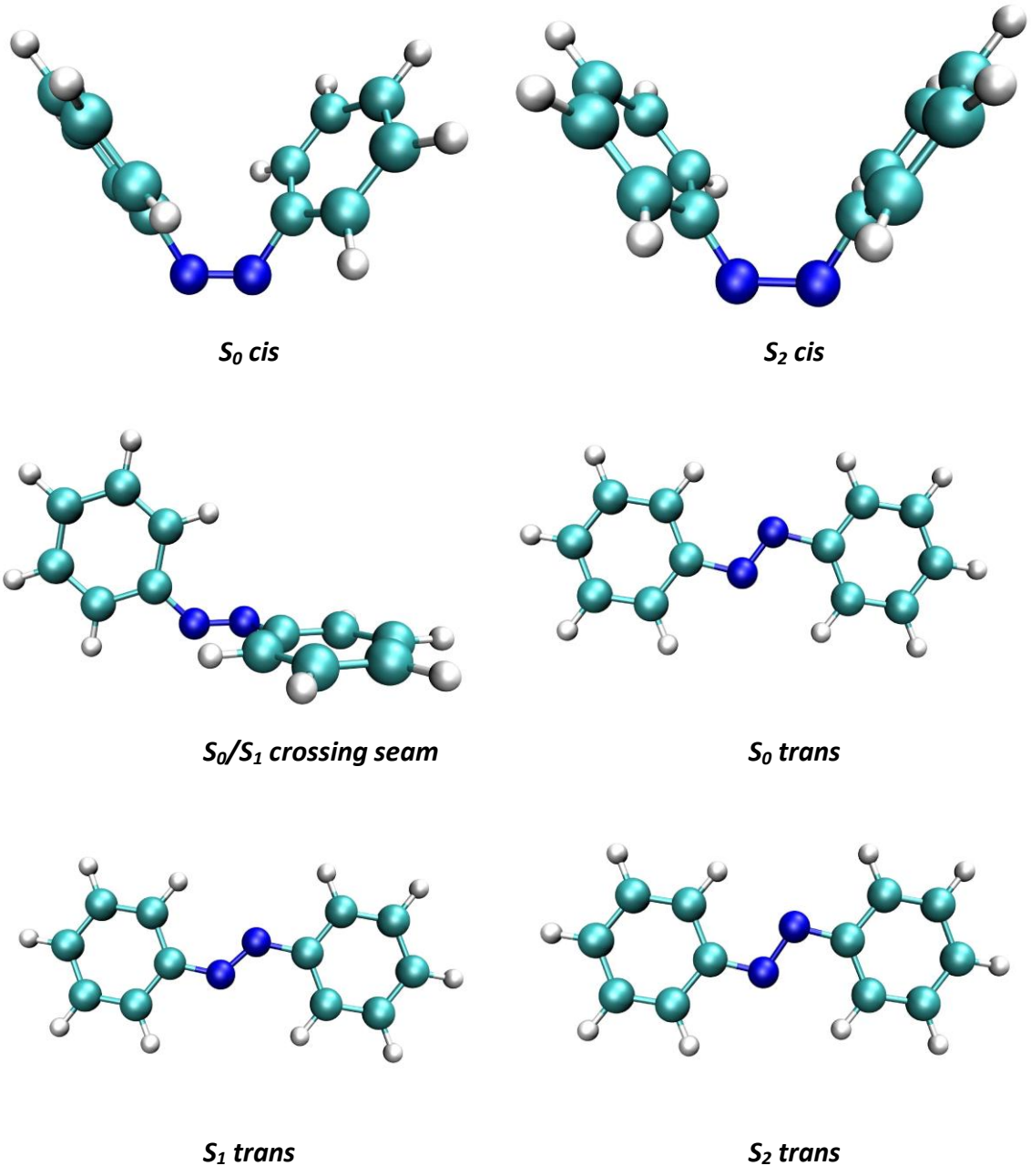

Figure 6: The optimized geometries of relevant structures

3.2.2 Ab initio molecular dynamics

Based on our results mentioned earlier we decided to run the molecular dynamics employing the Tully' least switches approach at the CASSCF (10, 8) level. The NEWTON-X package [37] was used for both creating the initial conditions and running the trajectories.

In NEWTON-X, the initial conditions are sampled in order to mimic the quantum wave-packet. Coordinates and momenta are sampled according to their probability distributions in a given harmonic vibrational state. Harmonic frequencies and normal modes were imported from the TURBOMOLE package. For the vibrational ground state, the initial conditions match the Wigner distribution for a quantum harmonic oscillator [38]

The initial conditions generator in NEWTON-X package also allowed us to simulate the UV absorption spectra (employing the Gaussian broadening method [38]), see figure 9.

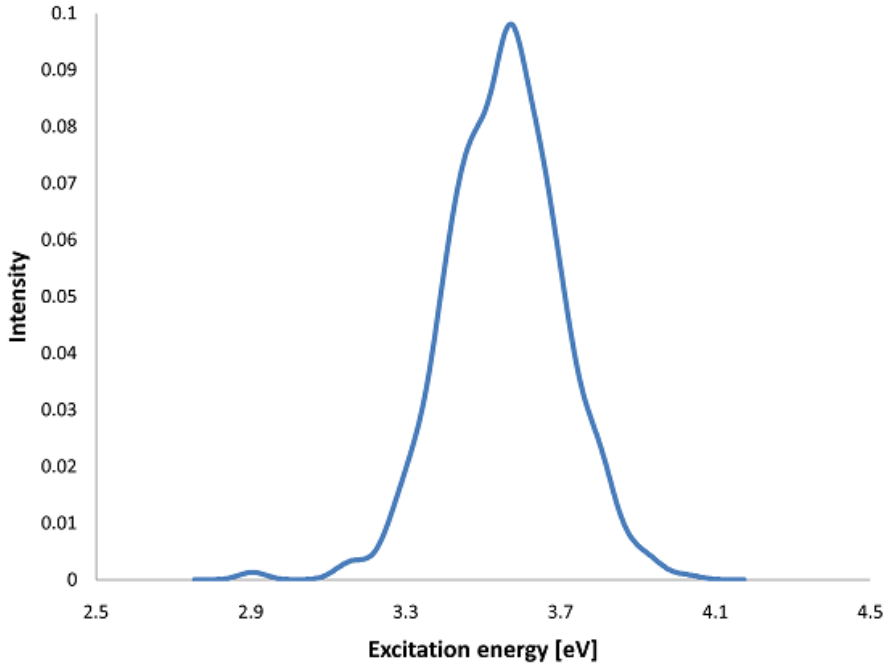

Figure 9: Excitation spectrum of cis-azobenzene

Two sets of trajectories were run, both with time step 0.5 fs and with maximal length of 500 fs. The first set, containing 50 trajectories, has employed the implementation of Röthlisberger's approach for approximation of the nonadiabatic coupling terms.

The second set contained 21 trajectories with same initial conditions already contained in the first set employing the analytical procedure for calculating the nonadiabatic couplings implemented in COLUMBUS package. This set of trajectories allows us to compare the result obtained within both approaches.

To compare the methods we investigated the average adiabatic populations of relevant states and the fractions of trajectories at a given state and time of the trajectory. Figure 10 shows the averaged adiabatic populations and fractions of trajectories for the S_1 state.

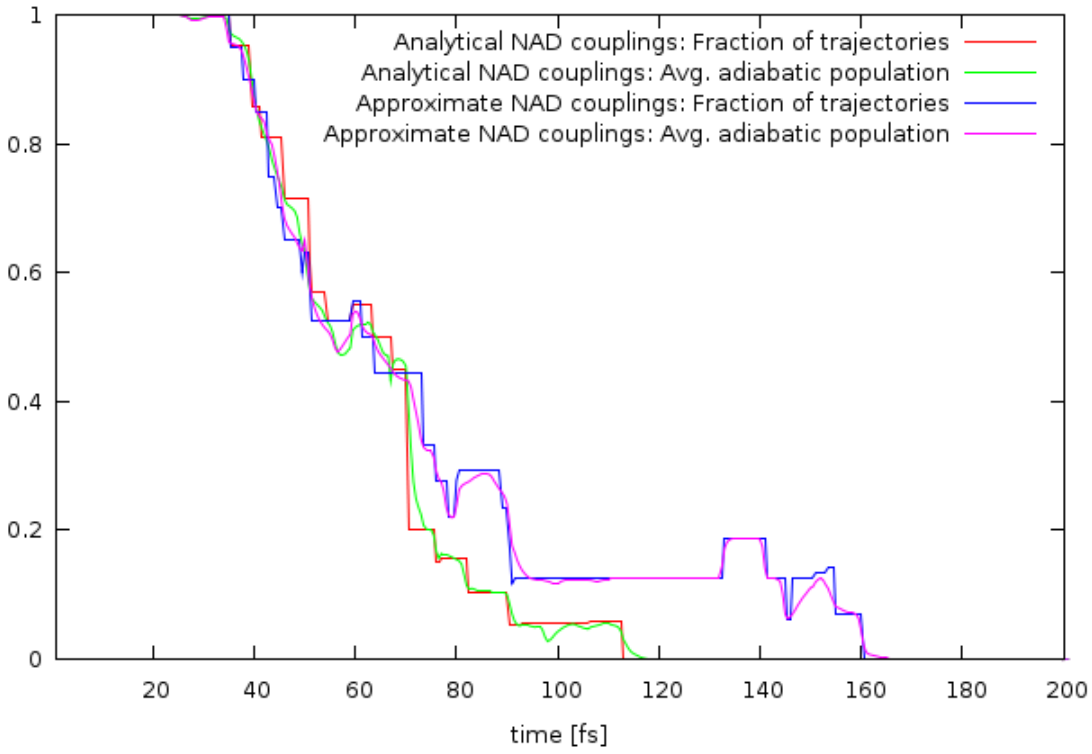

Figure 10: Comparison of two methods

Clearly, the plots closely correspond. The differences in the lower portion of Figure 10 are not statistically significant, as the number of actual trajectories in a given state gets very small.

In figure 11, we see a plot of the potential energies of the ground and first excited states of a typical trajectory:

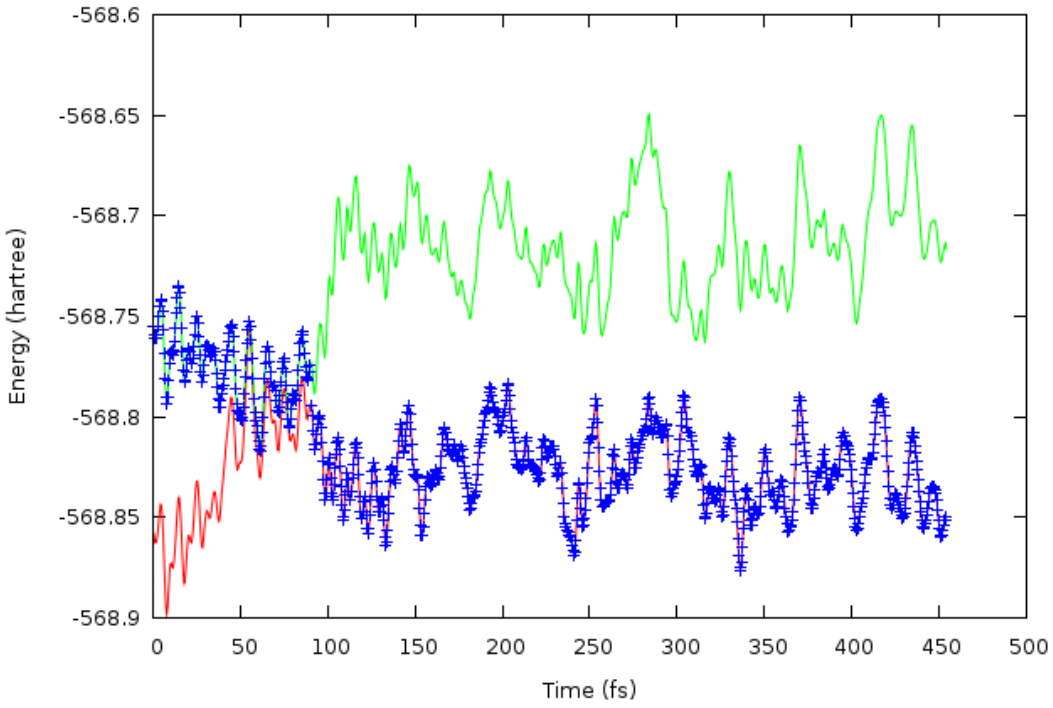

Figure 11: Potential energies of relevant states in a typical trajectory

(The crosses indicate the current state at each time step)

The actual isomerization is usually finished by 150 fs, as the molecule approaches the conical intersection located in the halfway reaction path in the interval between 40 and 100 fs. In figure 12, we can see the first part of a different trajectory. Very early (20-25 fs) the geometry approaches the crossing seam (this is indicated by the fact that the potential energy surfaces come close together) and continues to the conical intersection. After passing the conical intersection, the molecule remains in the ground state having large kinetic energy, which is slowly dissipated among all degrees of freedom.

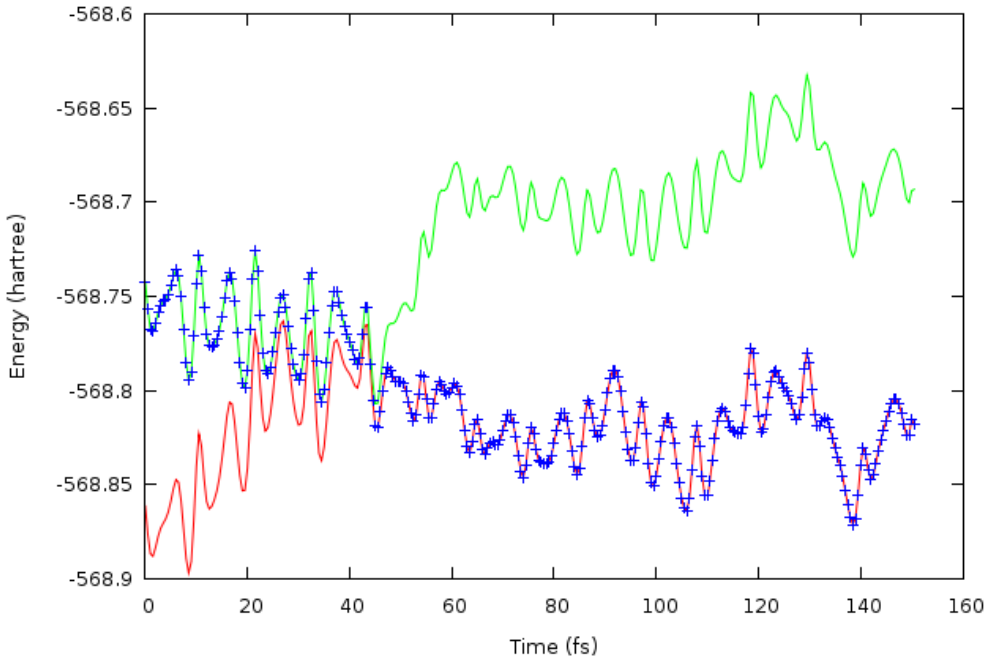

Figure 12: Potential energies of relevant states in a typical trajectory

(The crosses indicate the current state at each time step)

In the figure 13, we can see the average adiabatic populations and fraction of trajectories in the first excited state and the ground state as function of time.

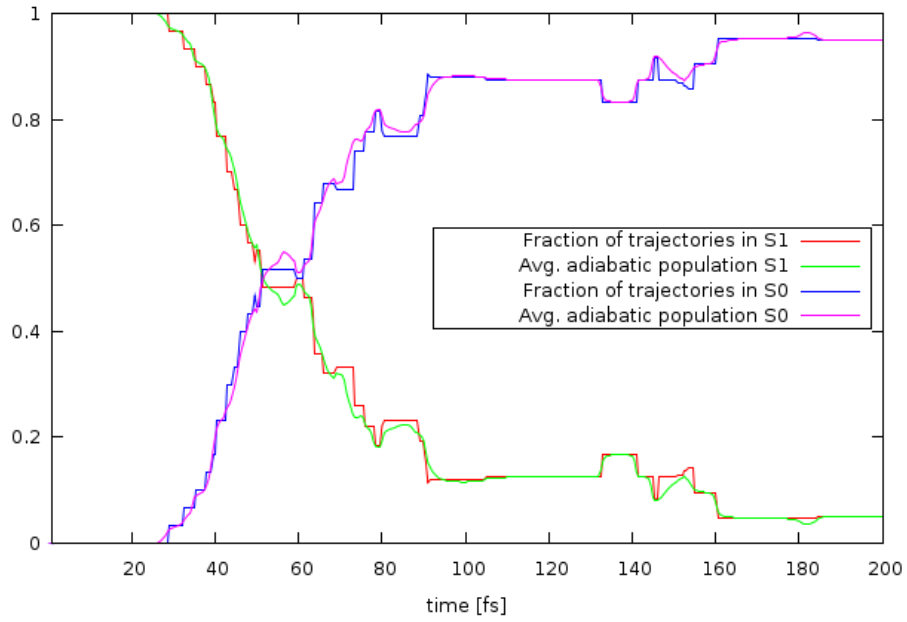

Figure 13: Potential energies of relevant states during isomerization

We can see that the fractions of trajectories closely correspond to the average adiabatic populations even for relatively small number of trajectories.

To verify the hypothesis that the isomerization is carried out through the rotational pathway we investigated the evolution of CNNC dihedral angle in time.

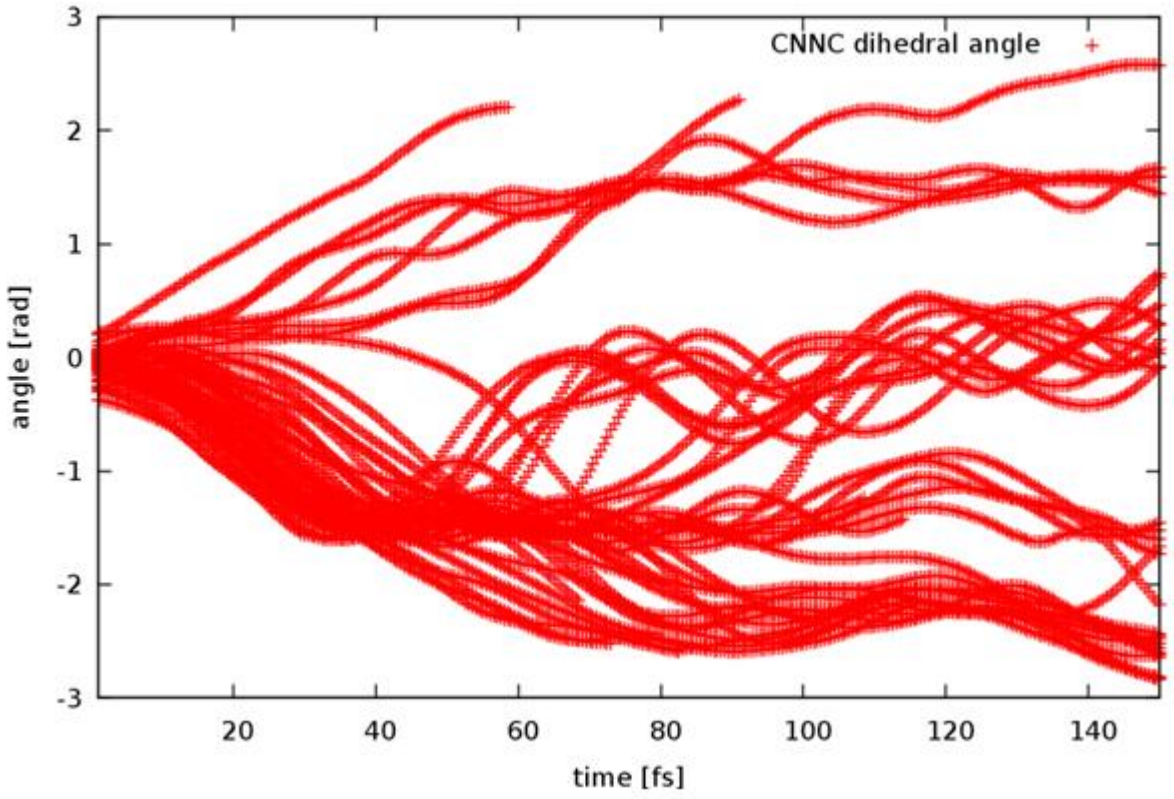

Figure 14: CNNC dihedral angle as a function of time

In figure 14, we can see that none of the trajectories remained planar in the process of isomerization, which excludes the inversion mechanism, and confirms the previous conclusions that rotational reaction mechanism dominates after the n-π excitation.

4 CONCLUSION

We have presented results of our recent work on the ab initio nonadiabatic molecular dynamics. We discussed the new efficient methods for approximating the non adiabatic couplings at the CASSCF and MR-CI levels and shown the recent applications of these methods on two molecular system.

First, we tested these methods on the Na_3F cluster and then we described an ab initio nonadiabatic MD simulation of the important cis-trans isomerization reaction of azobenzene.

We verified that the methods are capable of accurate description of the molecule by a series of single point calculations and geometry optimizations. We also found and optimized the conical intersection located in the middle of the rotational pathway.

We carried out 50 trajectories and showed that the reaction path of the photoisomerization reaction of azobenzene after the n-π excitation, starting in the cis isomer, goes through the conical intersection via the rotational pathway.

We also confirmed the accuracy of our approximations by submitting 20 trajectories with the same initial conditions employing analytical nonadiabatic couplings and obtaining similar results.

Our work on azobenzene photoisomerization will continue. We will continue with statistical analysis of our recent results and soon we will start investigating the dynamics staring in S_2 state and in near future also starting from the trans isomer. After that, we plan to add the effects of the solvent and also investigate bigger systems containing azobenzene structure with QM/MM methods.

5 REFERENCES

[1] B. J. Alder, T. E. Wainwright: J. Chem. Phys. **26**, 1208 (1957).

[2] R. Mitrić V. Bonačić–Koutecký, J. Pittner, H. Lischka: J. Chem. Phys. **125**, 24303 (2006).

[3] M. Born, R. Oppenheimer: Annalen der Physik **389,** 457 (1927).

[4] J. Fišer: Úvod do kvantové chemie, Praha: Academia (1983).

[5] R. Zahradník, R. Polák: Základy kvantové chemie, Praha: SNTL (1976)

[6] V. F. Bratcev: Dokl. Akad. Nauk **160,** 570 (1965).

[7] A. Szabo, N. S. Ostlund: Modern Quantum Chemistry: Introduction to Advanced Electronic Structure Theory, Dover (1996).

[8] C. G. Gray, G. Karl,V.A.Novikov: Progress in Classical and Quantum Variational Principles, Reports on Progress in Physics **67**, 159 (2004).

[9] M. W. Schmidt, M. S.Gordon: Annu. Rev. Phys. Chem. **49**, 233 (1998).

[10] B. O. Roos: Adv. Chem.Phys. **69**. 399 (1987).

[11] K. Ruedenberg, K.R. Sundberg: Quantum Science, New York: Plenum (1976).

[12] http://vergil.chemistry.gatech.edu/notes/ciscale/ciscale.html (30.8.2009).

[13] M. P. Allen, D. J. Tildesley: Computer Simulation of Liquids, Oxford University Press (1987).

[14] L. Verlet: Phys. Rev. **159**, 98 (1967).

[15] A. Bastida, C. Cruz, J. Zuniga, A. Requena. B. Miguel: Chemical Physics Letters **53**, 417 (2005).

[16] J. C. Tully: J. Chem. Phys. **93**, 1061 (1990).

[17] M. Ben-Nun, Jason Quenneville, J. Todd, J. Martínez: Phys. Chem. A **104** (2000).

[18] S. Hammes-Schiffer and J. C. Tully: J. Chem. Phys. **101**, 4657 (1994).

[19] E. Tapavicza, I. Tavernelli, U. Rothlisberger: Phys. Rev. Lett. **98**, 23001 (2007).

[20] J. Pittner, H. Lischka, M. Barbatti: Chem. Phys. **356**, 147 (2009)

[21] G. Granuci, M. Persico, A. Toniollo: J. Chem. Phys. **114**, 10608 (2001).

[22] V. Bonačić–Koutecký, J. Pittner, J. Koutecký: Chem. Phys. **210**, 313 (1996).

[23] C. Wang, S. Pollack, M.M. Kappes: Chem. Phys. Letters **26** (1990).

[24] J. M. L'Hermitea et al.: Eur. Phys. J. D **28**, 361 (2004).

[25] C. Ciminelli, G. Granucci, M. Persico: Chem. Eur. J. **10**, 2341 (2004).

[26] G. Granucci, M. Persico: Theor. Chem. Acc. **117**, 1131 (2007).

[27] T. Ishikawa, T. Noro, T. Shoda: J. Chem. Phys. **115**, 7503 (2001).

[28] E. W.-G. Diau: J. Phys. Chem. A **108**, 950 (2004).

[29] I. Conti, M. Garavelli, G. Orlandi: J. Am. Chem. Soc. **130**, 5216 (2008).

[30] H. Lischka, R. Shepard, I. Shavitt, R. M. Pitzer, M. Dallos, T. Müller, P. G. Szalay, F. B. Brown, R. Ahlrichs, H. J. Boehm, A. Chang, D. C. Comeau, R. Gdanitz, H. Dachsel, C. Ehrhardt, M. Ernzerhof, P. Höchtl, S. Irle, G. Kedziora, T. Kovar, V. Parasuk, M. J. M. Pepper, P. Scharf, H. Schiffer, M. Schindler, M. Schüler, M. Seth, E. A. Stahlberg, J.-G. Zhao, S. Yabushita, Z. Zhang, M. Barbatti, S. Matsika, M. Schuurmann, D. R. Yarkony, S. R. Brozell, E. V. Beck, J.-P. Blaudeau: COLUMBUS, an ab initio electronic structure program (2006).

[31] M. Hartmann, J. Pittner V. Bonačić–Koutecký: J. Chem. Phys. **114**, 2106 (2001).

[32] M. Hartmann, J. Pittner V. Bonačić–Koutecký: J. Chem. Phys. **114**, 2123 (2001).

[33] P. P. Birnbaum, J. H. Linford, D. W. G. Style: Trans. Faraday Soc. **49**, 735 (1953).

[34] D. L. Beveridge, H. H. Jaffe: J. Am. Chem. Soc. **88**, 1948 (1966).

[35] J. A. Bouwstra, A. Schouten, J. Kroon: Acta Crystallogr., Sect. C **39**,1121 (1983).

[36] T. Tsuji, H. Takashima, H. Takeuchi, T. Egawa, S. Konaka: J. Phys. Chem. A **105**, 9347 (2001).

[37] M. Barbatti, G. Granucci, M. Ruckenbauer, J. Pittner, M. Persico, H. Lischka: NEWTON-X: a package for Newtonian dynamics close to the crossing seam (2008).

[38] M. Barbatti, G. Granucci, M. Persico, M. Ruckenbauer, M. Vazdar, M. Eckert-Maksić, H. Lischka: J. Photochem. Photobio. A **190**, 228 (2007).